AIMS Mathematics, 8(8): 17719–17743.
DOI: 10.3934/math.2023905
Received: 17 March 2023
Revised: 15 May 2023
Accepted: 17 May 2023
Published: 24 May 2023

http://www.aimspress.com/journal/Math

Research article

Hopf bifurcation in a delayed reaction diffusion predator-prey model with weak Allee effect on prey and fear effect on predator

Fatao Wang, Ruizhi Yang, Yining Xie* and Jing Zhao

Northeast Forestry University, Harbin 150040, China

* **Correspondence:** Email: nefu_xieyining@163.com; Tel: +8618846035577.

Abstract: In this work, a Leslie-Gower model with a weak Allee effect on the prey and a fear effect on the predator is proposed. By using qualitative analyses, the local stability of the coexisting equilibrium and the existence of Turing instable are discussed. By analyzing the distribution of eigenvalues, the existence of a Hopf bifurcation is studied by using the gestation time delay as a bifurcation parameter. By utilizing the normal form method and the center manifold theorem, we calculate the direction of the Hopf bifurcation and the stability of bifurcating periodic solutions. We indicate that both the weak Allee effect on the prey and fear effect on the predator have an important impact on the dynamical behaviour of the new Leslie-Gower model. We also verify the obtained results by some numerical examples.

Keywords: predator-prey; fear effect; weak Allee effect; nonlocal competition; delay; Hopf bifurcation
Mathematics Subject Classification: 34K18, 35B32, 34K18, 34D23, 34H05, 35B32, 92D25

1. Introduction

One of the most important factors in ecology is the predator-prey interaction, which is usually complex and diverse. Scholars have long been committed to using mathematical methods to explain and predict it [1–7]. The population dynamics of predator and prey could easily be affected in nature [8–10]. In this work, we investigate a self-diffusive Leslie-Gower model with a time delay, fear effect on the predator, weak Allee effect, and nonlocal competition on the prey.

Many researchers only pay attention to the direct killing of prey by predators. However, with the development of society and the advancement of biomathematics, researchers [11–16] have a deeper understanding of the interactions between predator and prey, which are complex and multiple in nature. The existence of predators not only directly affects the density and growth rate of prey populations by eating prey, but also indirectly affects prey populations by influencing their dynamical behavior. Some

experiments have shown that prey will make various anti-predation responses to protect itself when it faces a predator, such as physiological changes, vigilance, foraging behavior. The phenomenon that the prey is always alert to possible attacks, is called fear effect. It is a physiological change related to the behavior and stress of a prey population in the presence of a predator.

Until now, most literatures have studied the fear effect on prey but few literatures have studied it on predator. Some scientists [17–19] have conducted experiments to study the fear effect on predators. They have found that the fear effect caused by a large predator could lead to a similar predation effect on medium-sized predators, leading the medium-sized predators to produce the anti-predation responses. This anti-predation behavior produced by the medium-sized predator will directly affect its consumption of prey. We can maintain the balance of the ecosystem by controlling the number of large predators to avoid excessive consumption of prey at the bottom of the food chain by the medium-sized predator.

When the density of the species population is low, the change law of the species population will be greatly affected by the internal mating of the population. W. Allee proposed the famous Allee effect for the first time [20]. Additionally, many scholars were concerned about the Allee effect in the predator-prey model [21–29]. Since the Allee effect usually occurs when the population density is either small or sparse. Thus, the Allee effects are strongly related to the extinction vulnerability of populations. The Allee effect is generally divided into either the strong or weak Allee effect. Whether the Allee effect is weak or strong depends on the opposing strengths of positive and negative density dependence. A strong Allee effect involves an Allee threshold. The Allee threshold is either a critical population size or a density below which the per capita population growth rate becomes negative. As mentioned in [23], the term $(u - m)$ is added to the logistic growth function $ru\left(1 - \frac{u}{K}\right)$ to investigate the influence of Allee threshold on prey. In [24], Courchamp revealed that studies of the strong Allee effect help support the relationship between the species populations at low densities and the population growth rate. Authors in [29] studied the following model:

$$\begin{cases} \dfrac{du}{dt} = ru\left(1 - \dfrac{u}{K}\right)(u - m) - \dfrac{cuv}{u + kv}, \\ \dfrac{dv}{dt} = \dfrac{ev}{1 + kv}\left(1 - \dfrac{v}{nu}\right). \end{cases} \tag{1.1}$$

Here u and v represent the prey and predator density, respectively. K, m, c, r, and e denote the environmental capacity, Allee threshold, maximal per capita consumption rate, and the intrinsic growth rates of the prey and predator, respectively. n is a measure of food quality that the prey provides for the conversion into predator birth. k measures the fear effect on the predator.

Unlike the strong Allee effect, there is no threshold for the weak Allee effect. Many literatures [30–32] have investigated the ecological model with the weak Allee effect. Authors in [21] have mentioned the following model:

$$\begin{cases} \dfrac{du}{dt} = ru\left(1 - \dfrac{u}{K}\right)\dfrac{u}{\beta + u} - \dfrac{cuv}{u + kv}, \\ \dfrac{dv}{dt} = \dfrac{ev}{1 + kv}\left(1 - \dfrac{v}{nu}\right), \end{cases} \tag{1.2}$$

where β is the weak Allee constant. Let $(u,\ v,\ t) = (K\bar{u},\ Kn\bar{v},\ \frac{\bar{t}}{r})$ and ignore the bar. Then, Eq (1.2)

becomes

$$\begin{cases} \dfrac{du}{dt} = u\left(\dfrac{(1-u)u}{b+u} - \dfrac{qv}{1+pv}\right), \\ \dfrac{dv}{dt} = \dfrac{sv}{1+pv}\left(1 - \dfrac{v}{u}\right), \end{cases} \tag{1.3}$$

where $b = \frac{\beta}{K}$, $q = \frac{Knc}{r}$, $p = Knk$, $s = \frac{e}{r}$.

In nature, due to the particularity of species breeding conditions and the necessity of gestational length, the species population density and birth rate of the species population at this stage are affected by the past period. Additionally, the energy conversion between predator and prey is not instantaneous. The influence of past history on the per capita growth rate of predators cannot be ignored [33–36]; therefore, we consider a time delay parameter τ for the predator-prey model. In addition, we assume that the distribution of population is uniform in model (1.3), which is generally not the situation in nature. In nature, due to the widespread self-diffusion phenomenon, few species populations have homogeneous spatial distribution [37–39]. Since the existence of diffusion phenomenon, the population model often shows some more abundant dynamic phenomena.

Another very important point is that the limited resources in nature makes the unlimited growth of species impossible, which will inevitably lead to competition among the prey population. Since the spatial distributions for the predator and prey population are inhomogeneous and disperse, this competition is usually nonlocal. Many scholars have studied the influence of it on the dynamic behavior of species [40–46]. In [47, 48], the authors modified the $\frac{u}{K}$ as $\frac{1}{K}\int_\Omega G(x,y)u(y,t)dy$ with some kernel function $G(x,y)$ to describe this competition. Due to the above factors, we added time delay and self-diffusion terms into Eq (1.3), and considered the nonlocal competition:

$$\begin{cases} \dfrac{\partial u(x,t)}{\partial t} = d_1\Delta u + u\left(\dfrac{(1-\int_\Omega G(x,y)u(y,t)dy)u}{b+u} - \dfrac{qv}{1+pv}\right), \\ \dfrac{\partial v(x,t)}{\partial t} = d_2\Delta v + \dfrac{sv}{1+pv}\left(1 - \dfrac{v(t-\tau)}{u(t-\tau)}\right), \quad u \in \Omega,\ t > 0, \\ \dfrac{\partial u(x,t)}{\partial \bar{\nu}} = \dfrac{\partial v(x,t)}{\partial \bar{\nu}} = 0, \quad x \in \partial\Omega,\ t > 0, \\ u(x,\theta) = u_0(x,\theta) \geq 0, v(x,\theta) = v_0(x,\theta) \geq 0, \quad x \in \bar{\Omega}, \theta \in [-\tau, 0]. \end{cases} \tag{1.4}$$

Here $\frac{\partial u(x,t)}{\partial t}$ and $\frac{\partial v(x,t)}{\partial t}$ represent the density gradients of the prey populations and predator populations, respectively. d_1, $d_2 > 0$ denote the diffusion coefficients of prey and predator, respectively. The notation Δ denotes the Laplace operator, and the notation Ω denotes a bounded domain with a smooth boundary $\partial\Omega$. τ describes either a gestation period or reaction time. The integral term $\int_\Omega G(x,y)u(y,t)dy$ in the first equation of (1.4) accounts for the nonlocal competition among the prey individuals. The kernel function is of the following form:

$$G(x,y) = \frac{1}{|\Omega|} = \frac{1}{l\pi}, \quad x, y \in \Omega,$$

which can be regarded as a measurement of the competition pressure at location x from the individuals at another location y. In this case, the competition strength among all prey individuals is the same across the habitat.

This paper mainly studies the significant effects of the weak Allee effect on prey and the fear effect on predators in the predator-prey system. We shall separately study the influence of the weak Allee effect and the fear effect on the spatial bifurcating periodic solutions.

This paper is organized as follows. In Section 2, we investigate the existence and stability of a coexisting equilibrium. In Section 3, we analyze the existence of a Hopf bifurcation. In Section 4, we consider the property of the Hopf bifurcation. In Section 5, we conduct a series of numerical simulations to illustrate the theoretical results. In Section 6, we elaborate a short conclusion.

2. Equilibria and stability

2.1. The existence of the equilibria

A discussion of the equilibria has been given in [21], but for the completeness of the paper, we still give the following lemma.

Lemma 2.1. *The equilibria of system* (1.4) *admit the following statements:*

(i) *The system* (1.4) *always has a distinct boundary equilibria given by* $\mathbb{E}_0(1,0)$ *for all positive parameters.*

(ii) *When* $bq > 1$ *and*

(ii*a*) *if* $p-q-1>0$ *and* $0<b<b^*$, *then system* (1.4) *has two positive equilibria* $\mathbb{E}_1(u_-,v_-)$ *and* $\mathbb{E}_2(u_+,v_+)$,

(ii*b*) *if* $p-q-1>0$ *and* $b=b^*$, *then system* (1.4) *has a unique positive equilibrium* $\mathbb{E}_3(u_3,v_3)$,

(ii*c*) *if* $p-q-1>0$, $b>b^*$ *or* $p-q-1\le 0$, *then system* (1.4) *has no positive equilibrium.*

(iii) *When* $bq = 1$ *and*

(iii*a*) *if* $p-q-1>0$, *then system* (1.4) *has a unique positive equilibrium* $\mathbb{E}_2(u_+,v_+)$,

(iii*c*) *if* $p-q-1\le 0$, *then system* (1.4) *has no positive equilibrium.*

(iv) *When* $0<bq<1$, *then system* (1.4) *has a unique positive equilibrium* $\mathbb{E}_2(u_+,v_+)$.

In the above, $b^* = \frac{(1+p+q)^2-4pq}{4pq}$, $u_\pm = v_\pm = \frac{(p-1-q)\pm\sqrt{(1-p+q)^2-4p(bq-1)}}{2p}$, and $u_3 = v_3 = \frac{(p-1-q)}{2p}$. Considering the biological significance of the system equilibrium, the rest of our discussion is focused on positive equilibrium.

Furthermore, we focus on the dynamics of system (1.3) in a neighbordhood of each equilibrium. Figure 1 shows the phase portraits of system (1.3) $b = 0.3$, $q = 0.9$, $p = 0.8$, and $s = 0.29$. The "green dot" represents the boundary point $\mathbb{E}_0$, the "blue dot" represents the equilibrium $\mathbb{E}_1$, and the "red dot" represents the unique positive equilibrium $\mathbb{E}_2$. By calculating, we obtain the real parts of eigenvalues of equilibrium $\mathbb{E}_2$ of -0.195771 and -0.195771. Therefore, the equilibrium $\mathbb{E}_2$ is a stable node. We selected the equilibrium point $\mathbb{E}_2$ for numerical simulations under the confirmed biological significance.

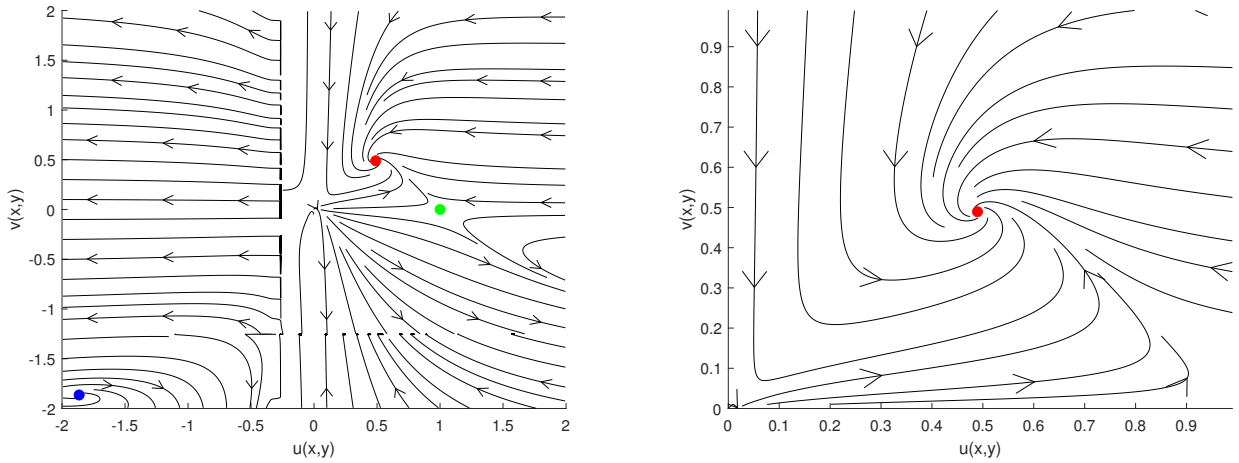

(a) **(b)**

Figure 1. The phase portraits of system (1.3) with $\tau = 0$, $b = 0.3$, $q = 0.9$, $p = 0.8$, $s = 0.29$, $d_1 = 0.18$ and $d_2 = 0.13$.

2.2. The stability analysis of the equilibria

Assume that $\Omega = (0, l\pi)$ and $G(x, y) = \frac{1}{l\pi}$. Let $\mathbb{N}$ denote the positive integer set, and $\mathbb{N}_0$ denote the nonnegative integer set. Without loss of generality, let us say that the positive equilibrium point is $E_*(u_*, v_*)$. Then, linearize system (1.4) at $E_*(u_*, v_*)$.

$$\frac{\partial}{\partial t}\begin{pmatrix} u(x,t) \\ u(x,t) \end{pmatrix} = D\begin{pmatrix} \Delta u(x,t) \\ \Delta v(x,t) \end{pmatrix} + J_1\begin{pmatrix} u(x,t) \\ v(x,t) \end{pmatrix} + J_2\begin{pmatrix} u(x,t-\tau) \\ v(x,t-\tau) \end{pmatrix} + J_3\begin{pmatrix} \hat{u}(x,t) \\ \hat{v}(x,t) \end{pmatrix}, \tag{2.1}$$

where

$$D = \begin{pmatrix} d_1 & 0 \\ 0 & d_2 \end{pmatrix}, \quad J_1 = \begin{pmatrix} a_{11} & a_{12} \\ 0 & a_{22} \end{pmatrix}, \quad J_2 = \begin{pmatrix} 0 & 0 \\ b_{21} & b_{22} \end{pmatrix}, \quad J_3 = \begin{pmatrix} \hat{a} & 0 \\ 0 & 0 \end{pmatrix},$$

$$a_{11} = -\frac{(1+2b)u^{*2}}{(b+u^*)^2} - \frac{u^{*3}}{(b+u^*)^2} + \frac{2u^*}{b+u^*} - \frac{qv^*}{1+pv^*}, \quad a_{12} = -\frac{qu^*}{(1+pv^*)^2} < 0, \quad a_{22} = \frac{s(u^*-v^*)}{u^*(1+pv^*)^2},$$

$$b_{21} = \frac{sv^{*2}}{u^{*2}(1+pv^*)} > 0, \quad b_{22} = -\frac{sv^*}{u^*(1+pv^*)} < 0, \quad \hat{a} = -\frac{u^{*2}}{b+u^*} < 0,$$

and $\hat{u} = \frac{1}{l\pi}\int_0^{l\pi} u(y,t)dy$.

Naturally, the characteristic equation is as follows:

$$\lambda^2 + A_n\lambda + B_n + (C_n - b_{22}\lambda)e^{-\lambda\tau} = 0, \quad n \in \mathbb{N}_0, \tag{2.2}$$

where

$$\begin{aligned} &A_0 = -(a_{11} + a_{22} + \hat{a}), \quad B_0 = a_{22}(\hat{a} + a_{11}), \quad C_0 = a_{11}b_{22} + \hat{a}b_{22} - a_{12}b_{21}, \\ &A_n = (d_1 + d_2)\frac{n^2}{l^2} - (a_{11} + a_{22}), \quad B_n = d_1d_2\frac{n^4}{l^4} - (a_{22}d_1 + a_{11}d_2)\frac{n^2}{l^2} + a_{11}a_{22}, \\ &C_n = -b_{22}d_1\frac{n^2}{l^2} + a_{11}b_{22} - a_{12}b_{21}, \quad n \in \mathbb{N}. \end{aligned} \tag{2.3}$$

Then, we make the following hypothesis:

($\mathbf{H_1}$) $(a_{11}+\hat{a})(a_{22}+b_{22}) > a_{12}b_{21},\ a_{11}+a_{22}+\hat{a}+b_{22}<0,\ A_n-b_{22}>0,\ B_n+C_n>0,$ for all $n\in\mathbb{N}$,

($\mathbf{H_2}$) $(a_{11}+\hat{a})(a_{22}+b_{22}) > a_{12}b_{21},\ a_{11}+a_{22}+\hat{a}+b_{22}<0,\ A_k-b_{22}<0$ (or $B_k+C_k<0$), for some $k\in\mathbb{N}$.

Furthermore, we come to the following situations.

Theorem 2.2. *Assume $\tau=0$. Then, the following statements are true for system* (2.1).
(i) *If* ($\mathbf{H_1}$) *holds, then $E_*(u_*,v_*)$ is locally asymptotically stable.*
(ii) *If* ($\mathbf{H_2}$) *holds, then $E_*(u_*,v_*)$ is Turing instable.*

Proof. Assume $\tau=0$, and then (2.2) becomes to

$$\lambda^2+(A_0-b_{22})\lambda+(B_0+C_0)=0 \tag{2.4}$$

and

$$\lambda^2+(A_n-b_{22})\lambda+(B_n+C_n)=0,\quad n\in\mathbb{N}. \tag{2.5}$$

When ($\mathbf{H_1}$) holds, the roots of Eqs (2.4) and (2.5) are all with negative real parts. Therefore, the equilibrium $E_*(u_*,v_*)$ is locally asymptotically stable. When ($\mathbf{H_2}$) holds, the roots of Eq (2.4) are all with negative real parts, but Eq (2.5) has at least one root with positive real part. Therefore, $E_*(u_*,v_*)$ is Turing unstable. □

Lemma 2.3. *If* ($\mathbf{H_1}$) *holds, then Eq* (2.5) *has a pair of purely imaginary roots $\pm i\omega_n$ at $\tau_n^j,\ j\in\mathbb{N}_0,\ n\in\mathbb{F}$, where*

$$\omega_n=\sqrt{\frac{1}{2}[-(A_n^2-2B_n-b_{22}^2)\pm\sqrt{(A_n^2-2B_n-b_{22}^2)^2-4(B_n^2-C_n^2)}]}, \tag{2.6}$$

and

$$\begin{aligned}
\tau_n^j&=\begin{cases}\frac{1}{\omega_n}\arccos(V_{cos}^{(n)})+2j\pi, & V_{sin}^{(n)}\geq 0,\\ \frac{1}{\omega_n}\left[2\pi-\arccos(V_{cos}^{(n)})\right]+2j\pi, & V_{sin}^{(n)}<0.\end{cases}\\
V_{cos}^{(n)}&=\frac{\omega^2(b_{22}A_n+C_n)-B_nC_n}{C_n^2+b_{22}^2\omega^2},\quad V_{sin}^{(n)}=\frac{\omega\left(A_nC_n+B_nb_{22}-b_{22}\omega^2\right)}{C_n^2+b_{22}^2\omega^2},\\
\mathbb{F}&=\{n|n\in\mathbb{M}_1\ or\ \mu_n=h^{\pm}\}\cup\{n|n\in\mathbb{M}_2\backslash\mathbb{M}_1,\ \mu_n\neq h^+,\ \mu_n\neq h^-\}.
\end{aligned} \tag{2.7}$$

Proof. We suppose $i\omega$ ($\omega>0$) is a solution of Eq (2.2), which leads to

$$-\omega^2+i\omega A_n+B_n+(C_n-b_{22}i\omega)e^{-i\omega\tau}=0,\quad n\in\mathbb{N}_0.$$

Then, separating the real and imaginary parts, we have

$$\begin{cases}A_n\omega=b_{22}\omega\cos\omega\tau+C_n\sin\omega\tau,\\ \omega^2-B_n=C_n\cos\omega\tau-b_{22}\omega\sin\omega\tau.\end{cases}$$

Thus, we can obtain

$$\cos\omega\tau = \frac{\omega^2(b_{22}A_n + C_n) - B_nC_n}{C_n^2 + b_{22}^2\omega^2}$$

and

$$\sin\omega\tau = \frac{\omega\left(A_nC_n + B_nb_{22} - b_{22}\omega^2\right)}{C_n^2 + b_{22}^2\omega^2}.$$

Due to $\cos^2\omega\tau + \sin^2\omega\tau = 1$, we have

$$\omega^4 + \omega^2\left(A_n^2 - 2B_n - b_{22}^2\right) + B_n^2 - C_n^2 = 0, \quad n \in \mathbb{N}_0. \tag{2.8}$$

Let $m = \omega^2$, then Eq (2.8) becomes

$$m^2 + m\left(A_n^2 - 2B_n - b_{22}^2\right) + B_n^2 - C_n^2 = 0, \quad n \in \mathbb{N}_0. \tag{2.9}$$

Let $P_n = A_n^2 - 2B_n - b_{22}^2$ and $Q_n = B_n^2 - C_n^2$. The roots of Eq (2.9) are $m^{\pm} = \frac{1}{2}[-P_n \pm \sqrt{P_n^2 - 4Q_n}]$. If $(\mathbf{H_1})$ holds, then $B_n + C_n > 0$ $(n \in \mathbb{N}_0)$.

Define

$$\begin{cases} h^{\pm} = \frac{a_{22}d_1 - b_{22}d_1 + a_{11}d_2 \pm \sqrt{-4(a_{11}a_{22} + a_{12}b_{21} - a_{11}b_{22})d_1d_2 + (-a_{22}d_1 + b_{22}d_1 - a_{11}d_2)^2}}{2d_1d_2}, \\ a^* = \frac{a_{22}^2d_1^2 - 2a_{22}b_{22}d_1^2 + b_{22}^2d_1^2 - 2a_{11}a_{22}d_1d_2 + 2a_{11}b_{22}d_1d_2 + a_{11}^2d_2^2}{4b_{21}d_1d_2}, \\ \mathbb{M}_1 = \{n | h^- < \mu_n < h^+,\ n \in \mathbb{N}\},\ \mu_n = \frac{n^2}{l^2}, \\ \mathbb{M}_2 = \{n | P_n < 0,\ P_n^2 - 4Q_n \geq 0,\ n \in \mathbb{N}\}. \end{cases}$$

Then, we have

$$\begin{cases} B_n - C_n < 0, & for\ a_{12} < a^*,\ n \in \mathbb{M}_1, \\ B_n - C_n \geq 0, & for\ a_{12} < a^*,\ n \notin \mathbb{M}_1, \\ B_n - C_n \geq 0, & for\ a_{12} \geq a^*,\ n \in \mathbb{N}. \end{cases}$$

Based on the above analysis, we will discuss the existence of purely imaginary roots of Eq (2.5) in the following three cases.

Case 1: $a_{12} > a^*$. For $n \in \mathbb{M}_2$, we can obtain that $m^{\pm} > 0$ if $P_n^2 - 4Q_n > 0$ and $m^+ = m^- > 0$ if $P_n^2 - 4Q_n = 0$. Then, Eq (2.5) has either one or two pairs of purely imaginary roots $\pm i\omega_n$ at $\tau_n^j,\ j \in \mathbb{N}_0$, where $i\omega_n^{\pm} = \sqrt{m^{\pm}}$.

Case 2: $a_{12} = a^*$. For $n \in \mathbb{M}_2 \backslash \mathbb{M}_1$, we can obtain that $m^{\pm} > 0$ if $P_n^2 - 4Q_n > 0$ and $m^+ = m^- > 0$ if $P_n^2 - 4Q_n = 0$ under the condition $\mu_n \neq h^+$ and $\mu_n \neq h^-$. Then, Eq (2.5) has either one or two pairs of purely imaginary roots $\pm i\omega_n$ at $\tau_n^j,\ j \in \mathbb{N}_0$. For $\mu_n = h^+$ or $\mu_n = h^-$, the Eq (2.5) has a pair of purely imaginary roots $\pm i\omega_n$ at $\tau_n^j,\ j \in \mathbb{N}_0$ when $P_n < 0$ and $P_n^2 - 4Q_n \geq 0$.

Case 3: $a_{12} < a^*$. For $n \in \mathbb{M}_2 \backslash \mathbb{M}_1$, we can obtain that $m^{\pm} > 0$ if $P_n^2 - 4Q_n > 0$ and $m^+ = m^- > 0$ if $P_n^2 - 4Q_n = 0$ under the condition $\mu_n \neq h^+$ and $\mu_n \neq h^-$. Then, Eq (2.5) has either one or two pairs of purely imaginary roots $\pm i\omega_n$ at $\tau_n^j,\ j \in \mathbb{N}_0$. For $\mu_n = h^+$ or $\mu_n = h^-$, Eq (2.5) has a pair of purely imaginary roots $\pm i\omega_n$ at $\tau_n^j,\ j \in \mathbb{N}_0$ when $P_n < 0$ and $P_n^2 - 4Q_n \geq 0$. For $n \in \mathbb{M}_1$, Eq (2.5) has a pair of purely imaginary roots $\pm i\omega_n$ at $\tau_n^j,\ j \in \mathbb{N}_0$ when $P_n^2 - 4Q_n \geq 0$.

Define

$$\mathbb{F} = \{n|n \in \mathbb{M}_1 \text{ or } \mu_n = h^{\pm}\} \cup \{n|n \in \mathbb{M}_2 \backslash \mathbb{M}_1,\ \mu_n \neq h^+,\ \mu_n \neq h^-\}.$$

$\mathbb{F}$ is a finite set obviously, since

$$\lim_{n\to\infty}(A_n^2 - 2B_n - b_{22}^2) \to +\infty,$$

$$\lim_{n\to\infty}(B_n - C_n) \to +\infty.$$

□

Lemma 2.4. *If* $(\mathbf{H_1})$ *is satisfied, then* $Re[\frac{d\lambda}{d\tau}|_{\tau=\tau_n^j}] > 0$ *for* $n \in \mathbb{F},\ j \in \mathbb{N}_0$ *are true.*

Proof. By Eq (2.2), we have

$$\left(\frac{d\lambda}{d\tau}\right)^{-1} = \frac{2\lambda + A_n - b_{22}e^{-\lambda\tau}}{(C_n - b_{22}\lambda)\lambda e^{-\lambda\tau}} - \frac{\tau}{\lambda}.$$

Then,

$$\begin{aligned}\left(\mathrm{Re}\left(\frac{d\lambda}{d\tau}\right)^{-1}\right)\Big|_{\tau=\tau_n^j} &= \mathrm{Re}\left(\frac{2\lambda + A_n - b_{22}e^{-\lambda\tau}}{(C_n - b_{22}\lambda)\lambda e^{-\lambda\tau}} - \frac{\tau}{\lambda}\right)\Big|_{\tau=\tau_n^j} \\ &= \left(\frac{1}{C_n^2 + b_{22}^2\omega^2}(2\omega^2 + A_n^2 - 2B_n - b_{22}^2)\right)\Big|_{\tau=\tau_n^j} \\ &= \left(\frac{1}{C_n^2 + b_{22}^2\omega^2}\sqrt{(A_n^2 - 2B_n - b_{22}^2)^2 - 4(B_n^2 - C_n^2)}\right)\Big|_{\tau=\tau_n^j} > 0.\end{aligned}$$

□

Then, we have the following theorem.

Theorem 2.5. *Assume* $(\mathbf{H_1})$ *are satisfied, the following statements are true for system* (1.4).
(i) $E_*(u_*, v_*)$ *is locally asymptotically stable for* $\tau \in [0, \tau_*)$, *where* $\tau_* = min\{\tau_n^0|\ n \in \mathbb{F}\}$.
(ii) $E_*(u_*, v_*)$ *is unstable for* $\tau \in [\tau_*, +\infty)$.
(iii) *The Hopf bifurcation values of system* (2.1) *are* $\tau = \tau^j$ *or* τ_n^j $(n \in \mathbb{F},\ j \in \mathbb{N}_0)$.

3. Property of Hopf bifurcation

In this section, we will give some conditions regarding the property of the Hopf bifurcation through the methods "the normal form theory" and "the center manifold theorem" in [40,41].

Denote $\tilde{\tau} = \tau_n^j$ for $j \in \mathbb{N}_0$ and $n \in \mathbb{F}$. Let $\bar{u}(x,t) = u(x,\tau t) - u_*$ and $\bar{v}(x,t) = v(x,\tau t) - v_*$. Then, system (1.4) (ignore the bar) becomes

$$\begin{cases}\dfrac{\partial u}{\partial t} = \tau\left(d_1\Delta u + (u+u^*)\left(\dfrac{\left(1 - \frac{1}{l\pi}\int_0^{l\pi}(u(y,t)+u^*)dy\right)(u+u^*)}{b+u+u^*} - \dfrac{q(v+v^*)}{1+p(v+v^*)}\right)\right), \\ \dfrac{\partial v}{\partial t} = \tau\left(d_2\Delta v + \dfrac{s(v+v^*)}{1+p(v+v^*)}\left(1 - \dfrac{v(t-1)+v^*}{u(t-1)+u^*}\right)\right).\end{cases} \tag{3.1}$$

System (3.1) can be rewritten in the following form:

$$\begin{cases} \dfrac{\partial u}{\partial t} =\tau[d_1\Delta u + a_{11}u + a_{12}v + \hat{a}\hat{u} + \alpha_1 u^2 + \hat{\alpha}_1 u\hat{u} + \alpha_2 uv + \alpha_3 v^2 + \alpha_4 u^3 + \hat{\alpha}_2 u^2\hat{u} \\ \qquad + \alpha_5 uv^2 + \alpha_6 v^3] + h.o.t., \\ \dfrac{\partial v}{\partial t} =\tau[d_2\Delta v + a_{22}v + b_{21}u(t-1) + b_{22}v(t-1) + \beta_1 u(t-1)v + \beta_2 v^2 + \beta_3 u^2(t-1) \\ \qquad + \beta_4 u(t-1)v(t-1) + \beta_5 vv(t-1) + \beta_6 v^3 + \beta_7 v^2 u(t-1) + \beta_8 v^2 v(t-1) \\ \qquad + \beta_9 vu^2(t-1) + \beta_{10}u^3(t-1) + \beta_{11}u^2(t-1)v(t-1)] + h.o.t., \end{cases} \tag{3.2}$$

where

$$a_{11} = -\frac{(1+2b)u^{*2}}{(b+u^*)^2} - \frac{u^{*3}}{(b+u^*)^2} + \frac{2u^*}{b+u^*} - \frac{qv^*}{1+pv^*}, \quad a_{12} = -\frac{qu^*}{(1+pv^*)^2}, \quad \hat{a} = -\frac{u^{*2}}{b+u^*},$$
$$\alpha_1 = -\frac{2b^2(u^*-1)}{(b+u^*)^3}, \quad \hat{\alpha}_1 = -\frac{u^*(2b+u^*)}{(b+u^*)^2}, \quad \alpha_2 = -\frac{q}{(1+pv^*)^2}, \quad \alpha_3 = \frac{2pqu^*}{(1+pv^*)^3},$$
$$\alpha_4 = \frac{6b^2(u^*-1)}{(b+u^*)^4}, \quad \hat{\alpha}_2 = -\frac{2b^2}{(b+u^*)^3}, \quad \alpha_5 = \frac{2pq}{(1+pv^*)^3}, \quad \alpha_6 = -\frac{6p^2qu^*}{(1+pv^*)^4},$$
$$a_{22} = \frac{s(u^*-v^*)}{u^*(1+pv^*)^2}, \quad b_{21} = \frac{sv^{*2}}{u^{*2}(1+pv^*)}, \quad b_{22} = -\frac{sv^*}{u^*+pu^*v^*}, \quad \beta_1 = \frac{sv^*}{(u^*+pu^*v^*)^2},$$
$$\beta_2 = -\frac{2ps(u^*-v^*)}{u^*(1+pv^*)^3}, \quad \beta_3 = -\frac{2sv^{*2}}{u^{*3}(1+pv^*)}, \quad \beta_4 = \frac{sv^*}{u^{*2}(1+pv^*)}, \quad \beta_5 = -\frac{s}{u^*(1+pv^*)^2},$$
$$\beta_6 = \frac{6p^2s(u^*-v^*)}{u^*(1+pv^*)^4}, \quad \beta_7 = -\frac{2psv^*}{u^{*2}(1+pv^*)^3}, \quad \beta_8 = \frac{2ps}{u^*(1+pv^*)^3}, \quad \beta_9 = -\frac{2sv^*}{u^{*3}(1+pv^*)^2},$$
$$\beta_{10} = \frac{6sv^{*2}}{u^{*4}(1+pv^*)}, \quad \beta_{11} = -\frac{2sv^*}{u^{*3}(1+pv^*)}.$$

Define a Hilbert space

$$X := \left\{(a,b)^T : (a,b) \in H^2(0,l\pi)\times H^2(0,l\pi),\ (\frac{\partial a}{\partial x}, \frac{\partial b}{\partial x})|_{x=0,l\pi} = 0\right\}.$$

The corresponding complexification $X_{\mathbb{C}}$ has the form $X_{\mathbb{C}} := X \oplus \mathrm{i}X = \{a + \mathrm{i}b |\ a,\ b \in X\}$. The complex-valued L^2 inner product is provided by $\langle a, b\rangle := \int_0^{l\pi}(\overline{a_1}b_1 + \overline{a_2}b_2)dx$, for $a = (a_1,\ a_2)^T$, $b = (b_1,\ b_2)^T \in X_{\mathbb{C}}$. Define a notation $\mathscr{C} := C([-1,0], X_{\mathbb{C}})$, which means the phase space with the sup norm, and we could write $\phi_t \in \mathscr{C}$, $\phi_t(\rho) = \phi(t+\rho)$ for $\rho \in [-1,0]$. Let $\chi_n^{(1)}(a) = (\gamma_n(a), 0)^T$, $\chi_n^{(2)}(a) = (0, \gamma_n(a))^T$ and $\chi_n = \{\chi_n^{(1)}(a), \chi_n^{(2)}(a)\}$, where $\{\chi_n^{(i)}(a)\}$ $(i = 1, 2)$ is an orthonormal basis of X. Define the subspace of $\mathscr{C}$, which is, $\mathscr{B}_n := \mathrm{span}\{\langle\phi(\cdot), \chi_n^{(j)}\rangle\chi_n^{(j)} | \phi \in \mathscr{C}, j = 1, 2\}$, $n \in \mathbb{N}_0$. According to the Riesz representation theorem, there exists a 2×2 matrix function $\eta_n(\theta, \tilde{\tau})$ of the bounded variation for $-1 \le \theta \le 0$, such that $-\tilde{\tau}D\frac{n^2}{l^2}\phi(0) + \tilde{\tau}L(\phi) = \int_{-1}^{0} d\eta_n(\theta,\tilde{\tau})\phi(\theta)$ for $\phi \in \mathscr{C}$. Define the bilinear form on $\mathscr{C}^*\times\mathscr{C}$, that is,

$$(\psi, \phi) = \psi(0)\phi(0) - \int_{-1}^{0}\int_{\zeta=0}^{\theta}\psi(\zeta-\theta)d\eta^n(\theta,\tilde{\tau})\phi(\zeta)d\zeta,\ \ for\ \phi \in \mathscr{C},\ \psi \in \mathscr{C}^*. \tag{3.3}$$

Define $\tau = \tilde{\tau} + \mu$. When $\mu = 0$, system Eq (3.2) undergoes a Hopf bifurcation at equilibrium $(0, 0)$, and the eigenfunctions has a pair of purely imaginary roots $\pm\mathrm{i}\omega_{n_0}$. $\mathscr{A}$ represents the infinitesimal generators

of the semigroup with $\mu = 0$ and $n = n_0$. The formal adjoint of $\mathscr{A}$ is denoted by $\mathscr{A}^*$, which is under the bilinear pairing Eq (3.3). Then, define the following Boolean function:

$$\delta(n_0) = \begin{cases} 1 & n_0 = 0, \\ 0 & n_0 \in \mathbb{N}. \end{cases} \tag{3.4}$$

Choose $\eta_{n_0}(0,\tilde{\tau}) = \tilde{\tau}(-n_0^2/l^2)D + \tilde{\tau}J_1 + \tilde{\tau}J_3\delta(n_{n_0})$, $\eta_{n_0}(-1,\tilde{\tau}) = -\tilde{\tau}J_2$, $\eta_{n_0}(\theta,\tilde{\tau}) = 0$ for $\theta \in (-1,0)$. Let $p(\sigma) = p(0)e^{\mathrm{i}\omega_{n_0}\tilde{\tau}\sigma}$ ($\sigma \in [-1,0]$) and $q(\theta) = q(0)e^{-\mathrm{i}\omega_{n_0}\tilde{\tau}\theta}$ ($\theta \in [0,1]$) be the eigenfunctions of $\mathscr{A}$ and $\mathscr{A}^*$ corresponding to the eigenvalue $i\omega_{n_0}\tilde{\tau}$, respectively. By calculation, we choose $p(0) = (1,p_1)^T$ and $q(0) = W(1,q_2)$, where $p_1 = \frac{1}{a_{12}}\left(-a_{11} + d_1\frac{n_0^2}{l^2} - \hat{a}\delta(n_0) + \mathrm{i}\omega_{n_0}\right)$, $q_2 = -\frac{a_{12}}{a_{22}+b_{22}e^{\mathrm{i}\tau\omega_{n_0}} - d_2\frac{n_0^2}{l^2} - \mathrm{i}\omega_{n_0}}$, and $W = (1 + p_1q_2 + \tilde{\tau}(b_{21}q_2 + b_{22}p_1q_2)e^{-\mathrm{i}\omega_{n_0}\tilde{\tau}})^{-1}$. Thus, system (3.1) becomes

$$\frac{dU(t)}{dt} = (\tilde{\tau}+\mu)D\Delta U(t) + (\tilde{\tau}+\mu)[J_1(U(t)) + J_2U(t-1) + J_3\hat{U}(t)] + G(\mu, U_t, \hat{U}_t), \tag{3.5}$$

where

$$G(\phi,\mu) = (\tilde{\tau}+\mu)\begin{pmatrix} \alpha_1\phi_1^2(0) + \hat{\alpha}_1\phi_1(0)\hat{\phi}_1(0) + \alpha_2\phi_1(0)\phi_2(0) + \alpha_3\phi_2^2(0) + \alpha_4\phi_1^3(0) + \hat{\alpha}_2\phi_1^2(0)\hat{\phi}_1(0) \\ +\alpha_5\phi_1(0)\phi_2^2(0) + \alpha_6\phi_2^3(0) \\ \beta_1\phi_1(-1)\phi_2(0) + \beta_2\phi_2^2(0) + \beta_3\phi_1^2(-1) + \beta_4\phi_1(-1)\phi_2(-1) + \beta_5\phi_2(0)\phi_2(-1) + \beta_6\phi_2^3(0) \\ +\beta_7\phi_1(-1)\phi_2^2(0) + \beta_8\phi_2^2\phi_2(-1) + \beta_9\phi_1^2(-1)\phi_2(0) + \beta_{10}\phi_1^3(-1) + \beta_{11}\phi_1^2(-1)\phi_2(-1) \end{pmatrix} \tag{3.6}$$

for $\phi = (\phi_1,\phi_2)^T \in \mathscr{C}$ and $\hat{\phi}_1 = \frac{1}{l\pi}\int_0^{l\pi}\phi_1 dx$. Then, we decompose the space $\mathscr{C}$ as $\mathscr{C} = \mathscr{P} \oplus \mathscr{Q}$, where $\mathscr{P} = \{ap\gamma_{n_0}(x) + \bar{a}\bar{p}\gamma_{n_0}(x) | a \in \mathbb{C}\}$, $\mathscr{Q} = \{\psi \in \mathscr{C} | (q\gamma_{n_0}(x),\psi) = 0 \text{ and } (\bar{q}\gamma_{n_0}(x),\psi) = 0\}$. Thus, system (3.6) becomes $U_t = f(t)p(\cdot)\gamma_{n_0}(x) + \bar{f}(t)\bar{p}(\cdot)\gamma_{n_0}(x) + \omega(t,\cdot)$ and $\hat{U}_t = \frac{1}{l\pi}\int_0^{l\pi}U_t dx$, where

$$f(t) = (q\gamma_{n_0}(x), U_t, \ \ \omega(t,\sigma) = U_t(\sigma) - 2\mathrm{Re}\{f(t)p(\sigma)\gamma_{n_0}(x)\}. \tag{3.7}$$

Then, we get $\dot{f}(t) = \mathrm{i}\omega_{n_0}\tilde{\tau}f(t) + \bar{q}(0) < G(0,U_t), \chi_{n_0} >$. There exists a center manifold $\mathscr{C}_0$ and we could write ω near $(0,0)$ as follows:

$$\omega(t,\sigma) = \omega(f(t),\bar{f}(t),\sigma) = \omega_{20}(\sigma)\frac{f^2}{2} + \omega_{11}(\sigma)f\bar{f} + \omega_{02}(\sigma)\frac{\bar{f}^2}{2} + \cdots. \tag{3.8}$$

Then, $\dot{f}(t) = \mathrm{i}\omega_{n_0}\tilde{\tau}f(t) + \varpi(f,\bar{f})$ is the system restricted to the center manifold C_0. Denote $\varpi(f,\bar{f}) = \varpi_{20}\frac{f^2}{2} + \varpi_{11}f\bar{f} + \varpi_{02}\frac{\bar{f}^2}{2} + \varpi_{21}\frac{f^2\bar{f}}{2} + \cdots$.

By direct computation, we have

$$\varpi_{20} = 2\tilde{\tau}W(\vartheta_1 + q_2\vartheta_2)I_3, \ \ \varpi_{11} = \tilde{\tau}W(\varrho_1 + q_2\varrho_2)I_3, \ \ \varpi_{02} = \bar{\varpi}_{20},$$

$$\varpi_{21} = 2\tilde{\tau}W[(\kappa_{11} + q_2\kappa_{21})I_2 + (\kappa_{12} + q_2\kappa_{22})I_4],$$

where

$$I_2 = \int_0^{l\pi}\gamma_{n_0}^2(x)dx,$$

$$I_3 = \int_0^{l\pi}\gamma_{n_0}^3(x)dx,$$

$$
\begin{aligned}
I_4 &= \int_0^{l\pi} \gamma_{n_0}^4(x)dx,\\
\vartheta_1 &= \alpha_1 + \hat{\alpha}_1\delta(n_0) + \alpha_2 p_1 + \alpha_3 p_1^2,\\
\vartheta_2 &= \beta_2 p_1^2 + e^{-i\tau\omega_{n_0}}(\beta_1 p_1 + \beta_5 p_1^2) + e^{-2i\tau\omega_{n_0}}(\beta_3 + \beta_4 p_1),\\
\varrho_1 &= \frac{1}{2}\alpha_1 + \frac{1}{2}\hat{\alpha}_1\delta(n_0) + \frac{1}{4}\alpha_2(\overline{p}_1 + p_1) + \frac{1}{2}\alpha_3\overline{p}_1 p_1,\\
\varrho_2 &= \frac{1}{2}\beta_2\overline{p}_1 p_1 + \frac{1}{2}\beta_3 + \frac{1}{4}\beta_4(p_1 + \overline{p}_1)\\
&\quad + \frac{1}{4}e^{-i\tau\omega_{n_0}}(\beta_1\overline{p}_1 + \beta_5\overline{p}_1 p_1) + \frac{1}{4}e^{i\tau\omega_{n_0}}(\beta_1 p_1 + \beta_5\overline{p}_1 p_1),\\
\kappa_{11} &= 2\omega_{11}^{(1)}(0)(2\alpha_1 + \hat{\alpha}_1\delta(n_0) + \hat{\alpha}_1 + \alpha_2 p_1) + 2\omega_{11}^{(2)}(0)(\alpha_2 + 2\alpha_3 p_1)\\
&\quad + \omega_{20}^{(1)}(0)(2\alpha_1 + \hat{\alpha}_1\delta(n_0) + \hat{\alpha}_1 + \alpha_2\overline{p}_1) + \omega_{20}^{(2)}(0)(\alpha_2 + 2\alpha_3\overline{p}_1) + \frac{3}{2}\hat{\alpha}_2\delta(n_0),\\
\kappa_{12} &= \frac{3}{2}\alpha_4 + \alpha_5\overline{p}_1 p_1 + \frac{1}{2}\alpha_5 p_1^2 + \frac{3}{2}\alpha_6\overline{p}_1 p_1^2,\\
\kappa_{21} &= 2\omega_{11}^{(1)}(-1)[\beta_1 p_1 + (\beta_4 p_1 + 2\beta_3)e^{-i\tau\omega_{n_0}}] + 2\omega_{11}^{(2)}(-1)(\beta_4 e^{-i\tilde{\tau}\omega_{n_0}}\\
&\quad + \beta_5 p_1) + \omega_{20}^{(1)}(-1)[(2\beta_3 + \beta_4\overline{p}_1)e^{i\tilde{\tau}\omega_{n_0}} + \beta_1\overline{p}_1] + \omega_{20}^{(2)}(-1)(\beta_4 e^{i\tilde{\tau}\omega_{n_0}} + \beta_5\overline{p}_1)\\
&\quad + 2\omega_{11}^{(2)}(0)[(\beta_1 + \beta_5 p_1)e^{-i\tilde{\tau}\omega_{n_0}} + 2\beta_2 p_1] + \omega_{20}^{(2)}(0)[(\beta_1 + \beta_5\overline{p}_1)e^{i\tilde{\tau}\omega_{n_0}} + 2\beta_2\overline{p}_1],\\
\kappa_{22} &= \beta_9 p_1 + \frac{3}{2}\beta_6\overline{p}_1 p_1^2 + e^{-i\tilde{\tau}\omega_{n_0}}(\frac{3}{2}\beta_{10} + \frac{1}{2}\beta_{11}\overline{p}_1 + \beta_{11}p_1 + \beta_7 p_1\overline{p}_1 + \beta_8 p_1^2\overline{p}_1)\\
&\quad + e^{i\tilde{\tau}\omega_{n_0}}(\frac{1}{2}\beta_7 p_1^2 + \frac{1}{2}\beta_8\overline{p}_1 p_1^2) + \frac{1}{2}\beta_9\overline{p}_1 e^{-2i\tilde{\tau}\omega_{n_0}}.
\end{aligned}
$$

Then, we should compute ω_{20} and ω_{11}. Due to Eq (3.7), we have

$$\dot{\omega} = \dot{U}_t - \dot{f}p\gamma_{n_0}(x) - \dot{\bar{f}}\bar{p}\gamma_{n_0}(x) = \mathscr{A}\omega + H(f, \bar{f}, \sigma), \tag{3.9}$$

where

$$H(f, \overline{f}, \sigma) = H_{20}(\sigma)\frac{f^2}{2} + H_{11}(\sigma)f\overline{f} + H_{02}(\sigma)\frac{\overline{f}^2}{2} + \cdots. \tag{3.10}$$

Comparing the coefficients of Eq (3.8) with Eq (3.9), we will get

$$(\mathscr{A} - 2\mathrm{i}\omega_{n_0}\tilde{\tau}I)\omega_{20}(\sigma) = -H_{20}(\sigma), \quad \mathscr{A}\omega_{11}(\sigma) = -H_{11}(\sigma). \tag{3.11}$$

Then, we have

$$
\begin{aligned}
\omega_{20}(\sigma) &= \frac{-\varpi_{20}}{\mathrm{i}\omega_{n_0}\tilde{\tau}}p(0)Q_{01} - \frac{\bar{\varpi}_{02}}{3\mathrm{i}\omega_{n_0}\tilde{\tau}}\bar{p}(0)Q_{02} + Q_1 e^{2\mathrm{i}\omega_{n_0}\tilde{\tau}\sigma},\\
\omega_{11}(\sigma) &= \frac{\varpi_{11}}{\mathrm{i}\omega_{n_0}\tilde{\tau}}p(0)Q_{01} - \frac{\bar{\varpi}_{11}}{\mathrm{i}\omega_{n_0}\tilde{\tau}}\bar{p}(0)Q_{02} + Q_2.
\end{aligned}
\tag{3.12}
$$

Denote $Q_{01} = e^{\mathrm{i}\omega_{n_0}\tilde{\tau}\sigma}\gamma_{n_0}(x)$, $Q_{02} = e^{-\mathrm{i}\omega_{n_0}\tilde{\tau}\sigma}\gamma_{n_0}(x)$, $Q_1 = \sum_{n=0}^{\infty} Q_1^{(n)}\gamma_{n_0}(x)$ and $Q_2 = \sum_{n=0}^{\infty} Q_2^{(n)}\gamma_{n_0}(x)$, and

Q_1 and Q_2 are described as follows:

$$Q_1^{(n)} = \left(2\mathrm{i}\omega_{n_0}\tilde{\tau}I - \int_{-1}^{0} e^{2\mathrm{i}\omega_{n_0}\tilde{\tau}\sigma} d\eta_{n_0}(\sigma,\bar{\tau})\right)^{-1} < \tilde{G}_{20}, \chi_n >,$$
$$Q_2^{(n)} = -\left(\int_{-1}^{0} d\eta_{n_0}(\sigma,\bar{\tau})\right)^{-1} < \tilde{G}_{11}, \chi_n >, \quad n \in \mathbb{N}_0,$$

$$< \tilde{G}_{20}, \chi_n >= \begin{cases} \frac{1}{l\pi}\hat{G}_{20}, & n_0 \neq 0, n = 0, \\ \frac{1}{2l\pi}\hat{G}_{20}, & n_0 \neq 0, n = 2n_0, \\ \frac{1}{l\pi}\hat{G}_{20}, & n_0 = 0, n = 0, \\ 0, & other, \end{cases}$$

$$< \tilde{G}_{11}, \chi_n >= \begin{cases} \frac{1}{l\pi}\hat{G}_{11}, & n_0 \neq 0, n = 0, \\ \frac{1}{2l\pi}\hat{G}_{11}, & n_0 \neq 0, n = 2n_0, \\ \frac{1}{l\pi}\hat{G}_{11}, & n_0 = 0, n = 0, \\ 0, & other, \end{cases}$$

where

$$\hat{G}_{20} = 2(\vartheta_1, \vartheta_2)^T, \ \hat{G}_{11} = 2(\varrho_1, \varrho_2)^T.$$

Therefore, we have

$$\begin{aligned} c_1(0) &= \frac{\mathrm{i}}{2\omega_n\tilde{\tau}}\left(\varpi_{20}\varpi_{11} - 2|\varpi_{11}|^2 - \frac{|\varpi_{02}|^2}{3}\right) + \frac{1}{2}\varpi_{21}, \quad \mu_2 = -\frac{\mathrm{Re}(c_1(0))}{\mathrm{Re}(\lambda'(\tilde{\tau}))}, \\ T_2 &= -\frac{\mathrm{Im}(c_1(0))}{\omega_{n_0}\tilde{\tau}} - \frac{\mu_2\mathrm{Im}(\lambda'(\tau_n^j))}{\omega_{n_0}\tilde{\tau}}, \quad \beta_2 = 2\mathrm{Re}(c_1(0)). \end{aligned} \tag{3.13}$$

Theorem 3.1. *For any critical value τ^j or τ_n^j ($n \in \mathbb{F}$, $j \in \mathbb{N}_0$), the following statements are true for system* (1.4).

(i) *If $\mu_2 > 0$ ($resp. < 0$), the Hopf bifurcation is forward* (*resp. backward*).

(ii) *If $\beta_2 < 0$ (resp. > 0), the bifurcation periodic solutions on the center manifold C_0 are orbitally asymptotically stable* (*resp. unstable*).

(iii) *If $T_2 > 0$ (resp. $T_2 < 0$), the Hopf bifurcation period increases* (*resp. decreases*).

4. Numerical simulations

4.1. The influence of the weak Allee effect

We analyze the effect of the parameter b, which is related to the weak Allee effect.

Fix parameters $q = 0.9$, $p = 0.8$, $s = 0.29$, $d_1 = 0.18$, and $d_2 = 0.13$. The bifurcation diagram of system (1.4) is given in Figure 2. From this diagram, we can obtain the relationship between the curves τ_0 and τ_1, and we can also obtain the intersecting point b^* ($b^* \approx 0.1727$).

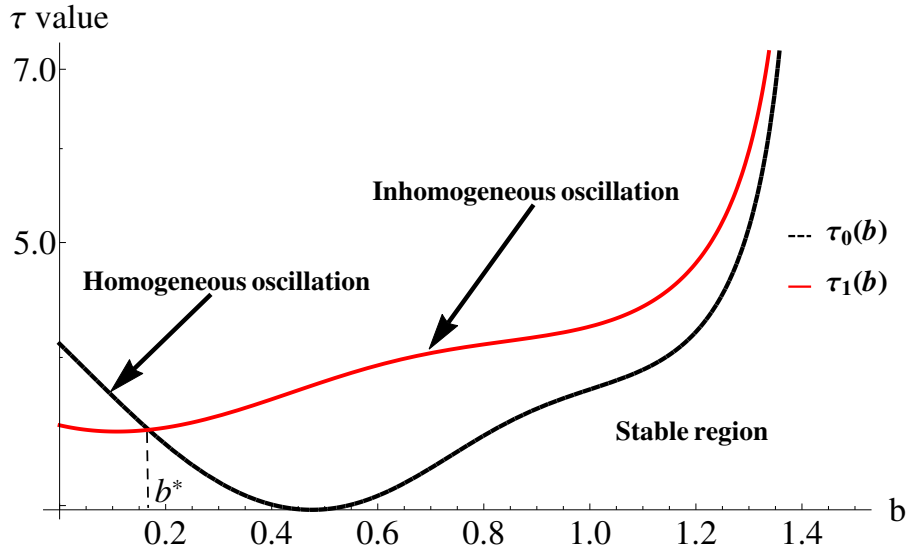

Figure 2. Bifurcation diagram of system (1.4) for b and τ with $q = 0.9$, $p = 0.8$, $s = 0.29$, $d_1 = 0.18$ and $d_2 = 0.13$.

Referring to the results of Figure 2, we can also observe that the spatial homogeneous periodic solution appears when $b > b^*$ and $\tau > \tau_0$, which may be asymptotically stable. The spatial inhomogeneous periodic solution appears when $b \in (0, b^*)$ and $\tau > \tau_1$, which may also be asymptotically stable. The stable steady state (u_*, v_*) will be reached at the rest.

Then, we select different parameter values to calculate and obtain some detailed values for properties of the Hopf bifurication (see Table 1). We found a phenomenon that a system with different parameters has different behaviors. Thus, we take six different sets of numbers and compare their different behaviors, which are summarized in Table 2. There will be three dynamic behaviors, namely asymptotically stable coexistence equilibrium (ASCE), stable spatially homogeneous periodic solutions (SSHPS), and stably spatially inhomogeneous periodic solutions (SSIPS).

Table 1. Some parameters for model (1.4) with different b.

b	(u_*, v_*)	τ_*	μ_2	β_2	T_2
0.1	(0.581419, 0.581419)	4.62517	109.505	−6.37427	−1.64733
0.3	(0.489427, 0.489427)	4.51241	237.19	−15.7077	−0.427416

Table 2. Numerical simulations for model (1.4).

b	τ	Model (1.4)	b	τ	Model (1.4)
0.1	3	ASCE (Figure 3)	0.3	3	ASCE (Figure 6)
0.1	4.8	SSIPS (Figure 4)	0.3	4.2	SSHPS (Figure 7)
0.1	5.2	SSIPS (Figure 5)	0.3	5.2	SSHPS (Figure 8)

Choose $b = 0.1$ and $\tau = 3$ ($\tau < \tau_1 < \tau_0$). The coexistence equilibrium (u_*, v_*) in system (1.4) is asymptotically stable (see the Figure 3).

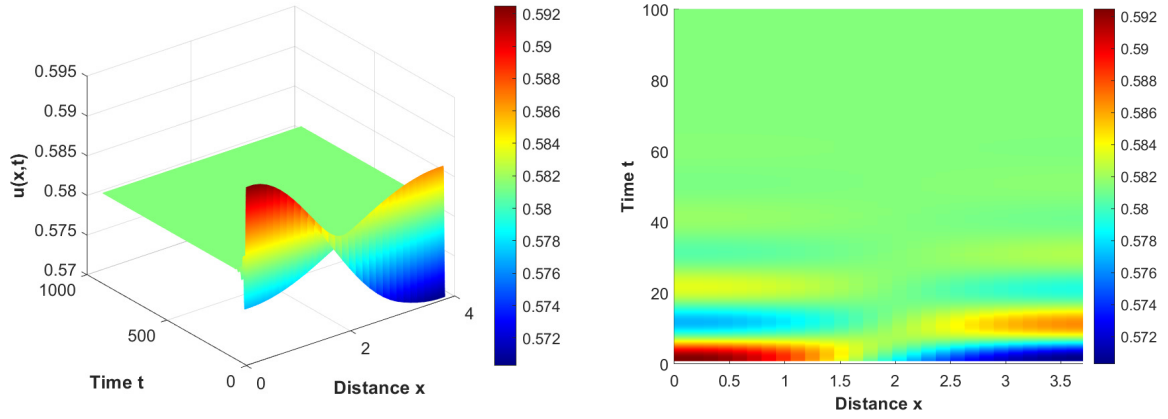

(a) (b)

Figure 3. Numerical simulations for prey population with $b = 0.1$, $\tau = 3$, $q = 0.9$, $p = 0.8$, $s = 0.29$, $d_1 = 0.18$ and $d_2 = 0.13$. (a) 1000 iterations, (b) 100 iterations.

Choose $b = 0.1$ and $\tau = 4.8$ ($\tau_1 < \tau < \tau_0$). As we can see from Figure 4, the coexistence equilibrium (u_*, v_*) is unstable, the spatial homogeneous periodic solution does not exist, and the stable spatial inhomogeneous periodic solution appears first. Therefore, we classify this equilibrium as a stable spatial inhomogeneous periodic solution.

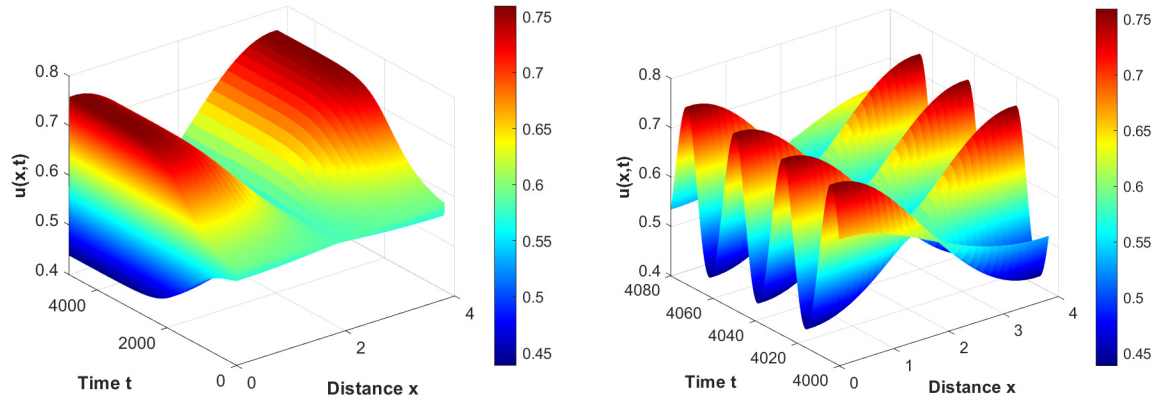

(a) (b)

Figure 4. Numerical simulations for prey population with $b = 0.1$, $\tau = 4.8$, $q = 0.9$, $p = 0.8$, $s = 0.29$, $d_1 = 0.18$ and $d_2 = 0.13$. (a) 4500 iterations, (b) from 4000 iterations to 4080 iterations.

Choose $b = 0.1$ and $\tau = 5.2$ ($\tau_1 < \tau_0 < \tau$). As we can see from Figure 5, the coexistence equilibrium (u_*, v_*) is unstable, and the spatial homogeneous periodic solution appears first, though is not stable. Thus, system (1.4) has a stable spatial inhomogeneous periodic solution.

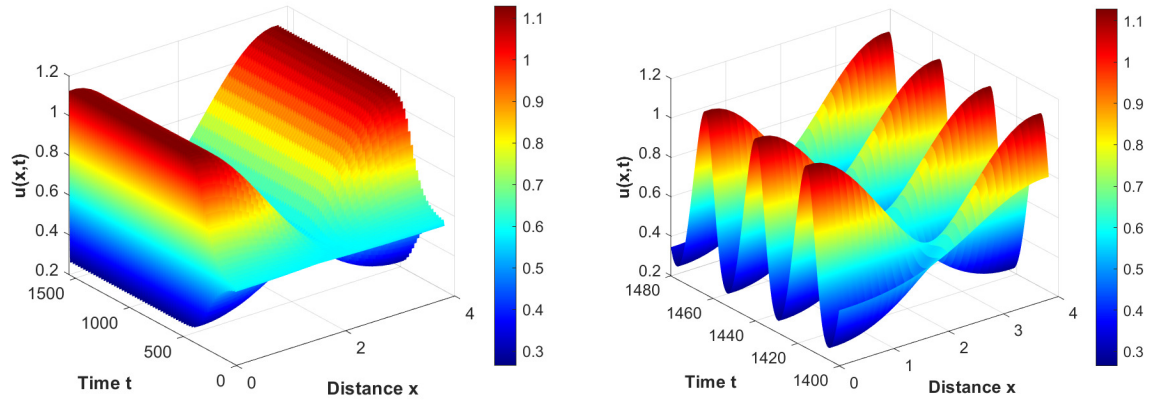

(a) (b)

Figure 5. Numerical simulations for prey population with $b = 0.1$, $\tau = 5.2$, $q = 0.9$, $p = 0.8$, $s = 0.29$, $d_1 = 0.18$ and $d_2 = 0.13$. (a) 1500 iterations, (b) from 1400 iterations to 1480 iterations.

Choose $b = 0.3$ and $\tau = 3$ ($\tau < \tau_0 < \tau_1$). As we can see from Figure 6, the coexistence equilibrium $(u_*,\ v_*)$ is asymptotically stable. Comparing detail diagrams between Figures 3(b) and 6(b), we can find that the coexistence equilibrium (u^*, v^*) with a lager weak Allee effect becomes stable faster and has a smaller amplitude. Thus, we can conclude that the existence of the weak Allee effect term is beneficial to the stability of the coexistence equilibrium.

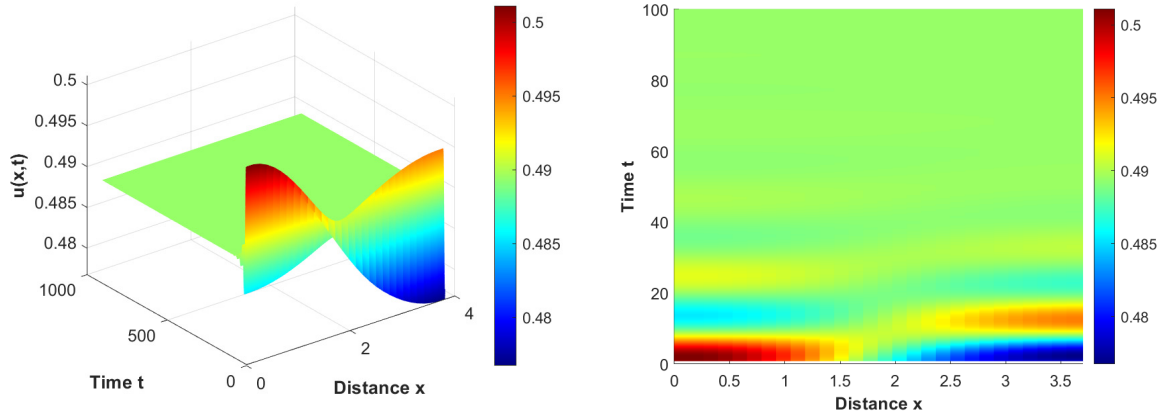

(a) (b)

Figure 6. Numerical simulations for prey population with $b = 0.3$, $\tau = 3$, $q = 0.9$, $p = 0.8$, $s = 0.29$, $d_1 = 0.18$ and $d_2 = 0.13$. (a) 1000 iterations, (b) 100 iterations.

Choose $b = 0.3$ and $\tau = 4.2$ ($\tau_0 < \tau < \tau_1$). As we can see from Figure 7, the coexistence equilibrium $(u_*,\ v_*)$ is unstable, the spatial inhomogeneous periodic solution does not exist, and the stable spatial homogeneous periodic solution appears first. Therefore, we classify this equilibrium as a stable spatial homogeneous periodic solution.

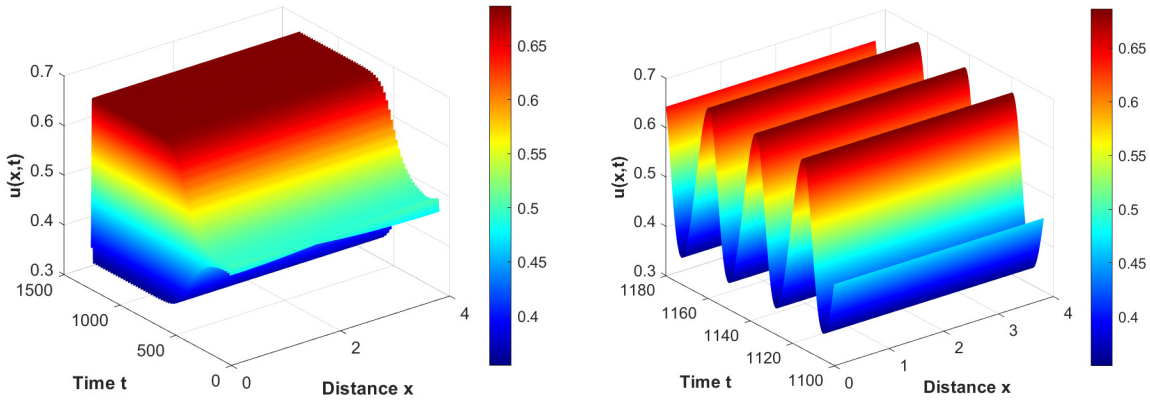

(a) (b)

Figure 7. Numerical simulations for prey population with $b = 0.3$, $\tau = 4.2$, $q = 0.9$, $p = 0.8$, $s = 0.29$, $d_1 = 0.18$ and $d_2 = 0.13$. (a) 1500 iterations, (b) from 1100 iterations to 1180 iterations.

Choose $b = 0.3$ and $\tau = 5.2$ ($\tau_0 < \tau_1 < \tau$). As we can see from Figure 8, the coexistence equilibrium (u_*, v_*) is unstable, and the spatial inhomogeneous periodic solution appears first, though is not stable. The system (1.4) has stable spatial homogeneous periodic solution. Comparing detail diagrams between Figures 5(b) and 8(b), we can find that the weak Allee effect term has a slight effect on the solution but does not affect its stability. The period of the coexistence equilibrium (u^*, v^*) with a lager weak Allee effect has increased and has a smaller amplitude. It can be seen that the weak Allee effect can affect the homogeneity of the periodic solution.

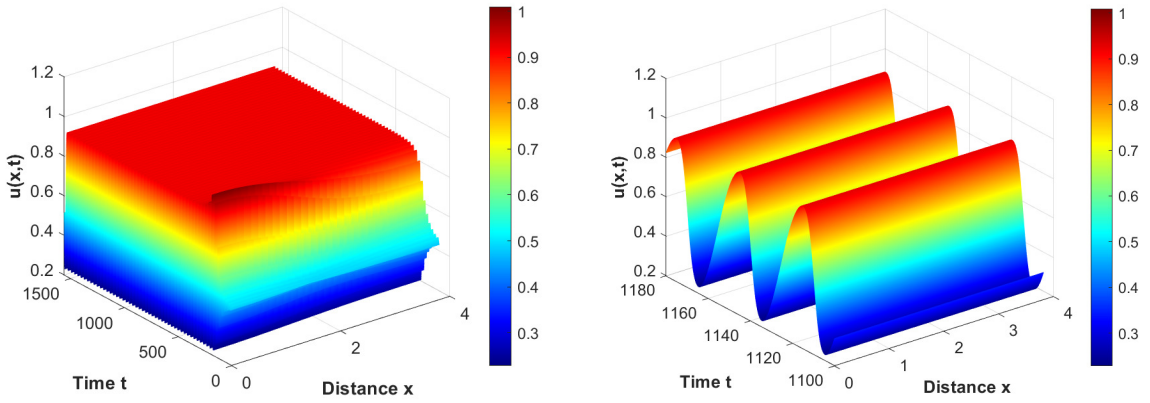

(a) (b)

Figure 8. Numerical simulations for prey population with $b = 0.3$, $\tau = 5.2$, $q = 0.9$, $p = 0.8$, $s = 0.29$, $d_1 = 0.18$ and $d_2 = 0.13$. (a) 1500 iterations, (b) from 1100 iterations to 1180 iterations.

4.2. The influence of fear effect

We analyze the effect of parameter p, which is related to the fear effect.

Fix parameters $q = 0.45$, $b = 0.1$, $s = 0.25$, $d_1 = 0.13$, and $d_2 = 0.2$. The bifurcation diagram of system (1.4) is given in Figure 9. In the diagram, the curves of τ_0 and τ_1 intersect at the points p^*, where $p^* \approx 0.3059$.

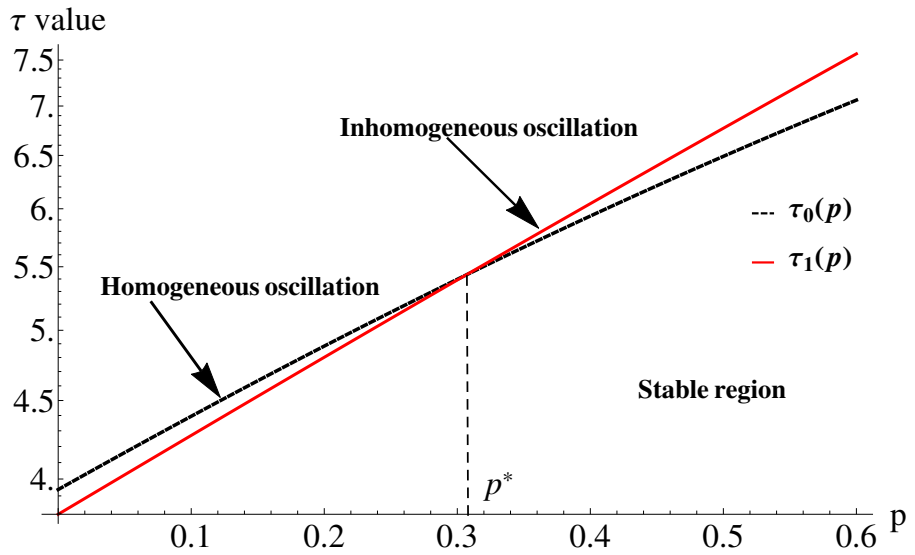

Figure 9. Bifurcation diagram of system (1.4) for p and τ with $q = 0.45$, $b = 0.1$, $s = 0.25$, $d_1 = 0.13$ and $d_2 = 0.2$.

Referring to the results of Figure 9, we can also observe that the spatial homogeneous periodic solution appears when $p > p^*$ and $\tau > \tau_0$, which may be asymptotically stable. The spatial inhomogeneous periodic solution appears when $p \in (0, p^*)$ and $\tau > \tau_1$, which may also be asymptotically stable. The stable steady state (u_*, v_*) will be reached at the rest.

Then, we select different parameter values to calculate and obtain some detailed values for the Hopf bifurcation properties (see Table 3). We took six different sets of numbers and compared their behavior, which are summarized into Table 4.

Table 3. Some parameters for model (1.4) with different p.

p	(u_*, v_*)	τ_*	μ_2	β_2	T_2
0.05	(0.666288, 0.666288)	4.02552	44.1971	−3.56918	1.19861
0.56	(0.734021, 0.734021)	7.24064	8.91317	−0.222507	−1.38483

Table 4. Numerical simulations for model (1.4).

p	τ	Model (1.4)	p	τ	Model (1.4)
0.05	3.9	ASCE (Figure 10)	0.56	6.5	ASCE (Figure 13)
0.05	4.15	SSIPS (Figure 11)	0.56	7.01	SSHPS (Figure 14)
0.05	4.2	SSIPS (Figure 12)	0.56	7.5	SSHPS (Figure 15)

Choose $p = 0.05$ and $\tau = 3.9$ ($\tau < \tau_1 < \tau_0$). As we can see from Figure 10, the coexistence equilibrium (u_*, v_*) is asymptotically stable.

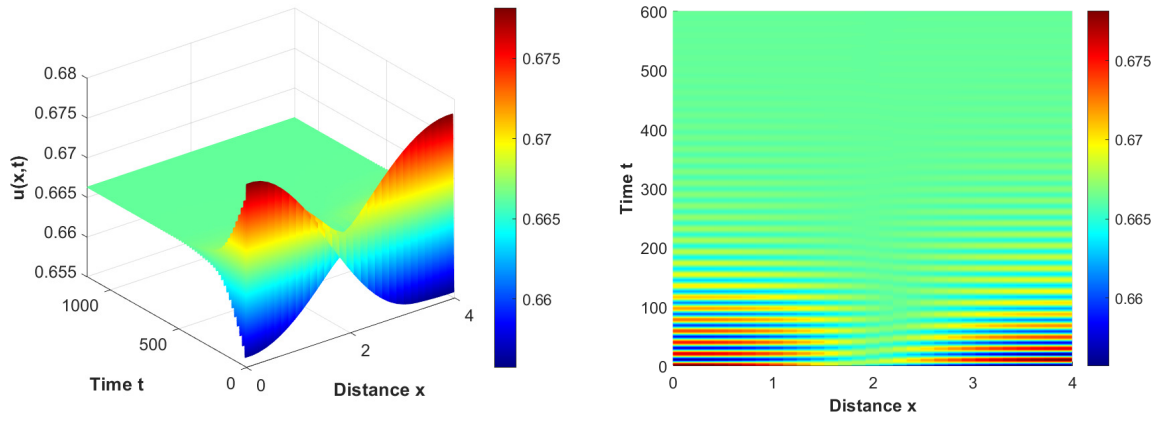

(a) (b)

Figure 10. Numerical simulations for prey population with $p = 0.05$, $\tau = 3.9$, $q = 0.45$, $b = 0.1$, $s = 0.25$, $d_1 = 0.13$ and $d_2 = 0.2$. (a) 1200 iterations, (b) 600 iterations.

Choose $p = 0.05$ and $\tau = 4.15$ ($\tau_1 < \tau < \tau_0$). As we can see from Figure 11, the coexistence equilibrium (u_*, v_*) is unstable, the spatial homogeneous periodic solution does not exist, and the stable spatial inhomogeneous periodic solution appears first. Therefore, we classify this equilibrium as a stable spatial inhomogeneous periodic solution.

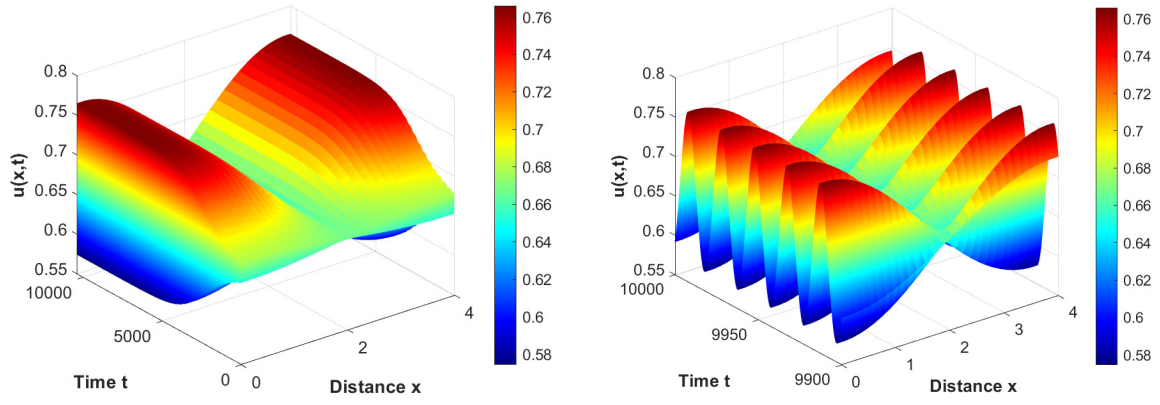

(a) (b)

Figure 11. Numerical simulations for prey population with $p = 0.05$, $\tau = 4.15$, $q = 0.45$, $b = 0.1$, $s = 0.25$, $d_1 = 0.13$ and $d_2 = 0.2$. (a) 10375 iterations, (b) from 9900 iterations to 10000 iterations.

Choose $p = 0.05$ and $\tau = 4.2$ ($\tau_1 < \tau_0 < \tau$). As we can see from Figure 12, the coexistence equilibrium (u_*, v_*) is unstable, and the spatial homogeneous periodic solution appears first, though is not stable. Thus, system (1.4) has stable spatial inhomogeneous periodic solution.

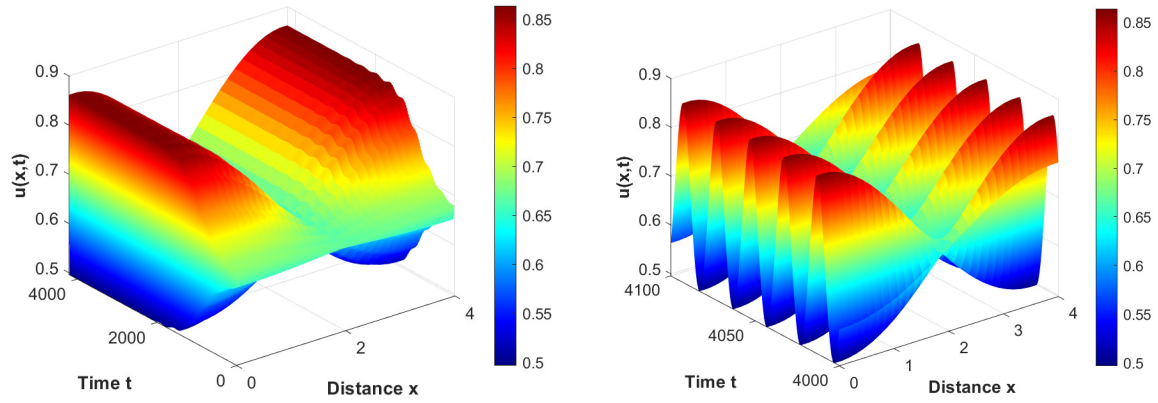

(a) (b)

Figure 12. Numerical simulations for prey population with $p = 0.05$, $\tau = 4.2$, $q = 0.45$, $b = 0.1$, $s = 0.25$, $d_1 = 0.13$ and $d_2 = 0.2$. (a) 4200 iterations, (b) from 4000 iterations to 4100 iterations.

Choose $p = 0.56$ and $\tau = 6.5$ ($\tau < \tau_0 < \tau_1$). As we can see from Figure 13, the coexistence equilibrium (u_*, v_*) is asymptotically stable. Comparing detail diagrams between Figures 10(b) and 13(b), we can find that the coexistence equilibrium (u^*, v^*) with a lager fear effect becomes stable slower and has a larger amplitude. Thus, we can conclude that the existence of the fear effect term is not beneficial to the stability of the coexistence equilibrium.

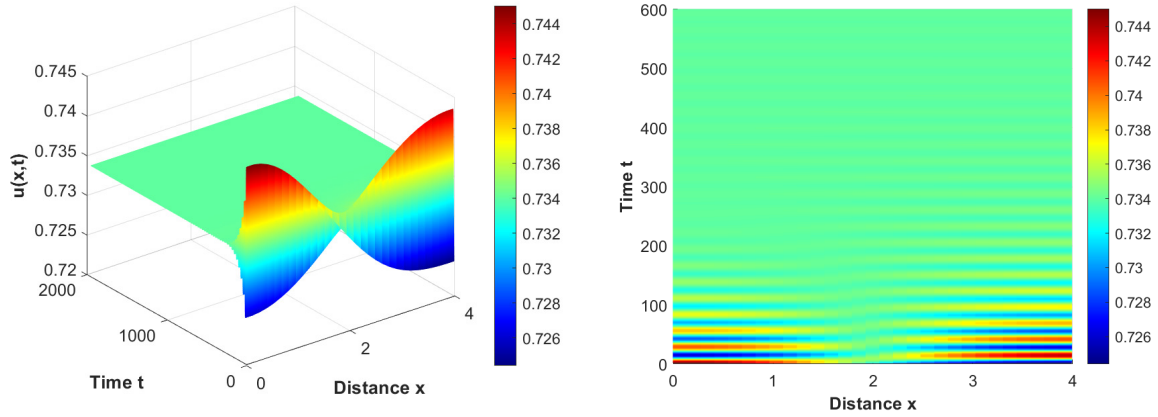

(a) (b)

Figure 13. Numerical simulations for prey population with $p = 0.56$, $\tau = 6.5$, $q = 0.45$, $b = 0.1$, $s = 0.25$, $d_1 = 0.13$ and $d_2 = 0.2$. (a) 2000 iterations, (b) 600 iterations.

Choose $p = 0.56$ and $\tau = 4.15$ ($\tau_0 < \tau < \tau_1$). As can be seen in Figure 14, the coexistence equilibrium (u_*, v_*) is unstable, the spatial inhomogeneous periodic solution does not exist, and the stable spatial homogeneous periodic solution appears first. Therefore, we classify this equilibrium as a stable spatial homogeneous periodic solution.

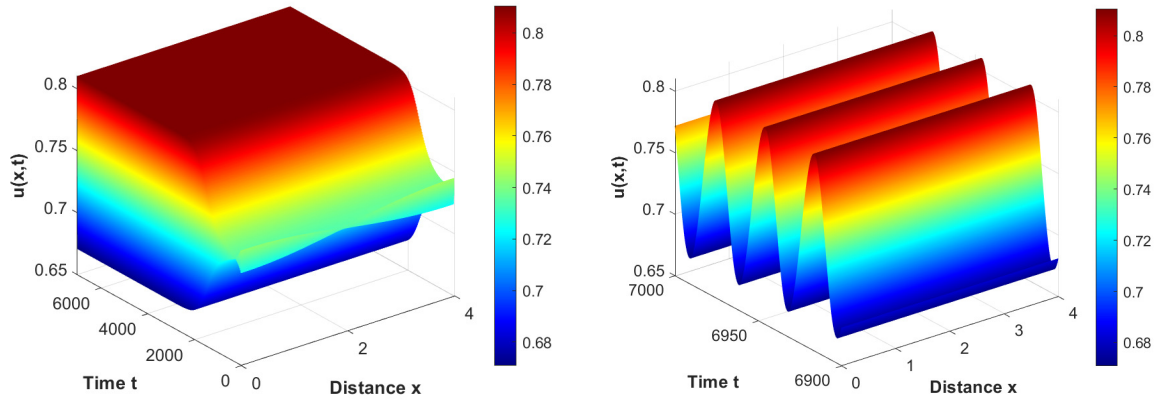

(a) (b)

Figure 14. Numerical simulations for prey population with $p = 0.56$, $\tau = 7.01$, $q = 0.45$, $b = 0.1$, $s = 0.25$, $d_1 = 0.13$ and $d_2 = 0.2$. (a) 7010 iterations, (b) from 6900 iterations to 7000 iterations.

Choose $p = 0.56$ and $\tau = 4.2$ ($\tau_0 < \tau_1 < \tau$). As can be seen in Figure 15, the coexistence equilibrium (u_*, v_*) is unstable, and the spatial inhomogeneous periodic solution appears first, though is not stable. The system (1.4) has a stable spatial homogeneous periodic solution. We can find that the fear effect term has a slight effect on the solution and does not affect its stability. Additionally, it can affect the homogeneity of the periodic solution.

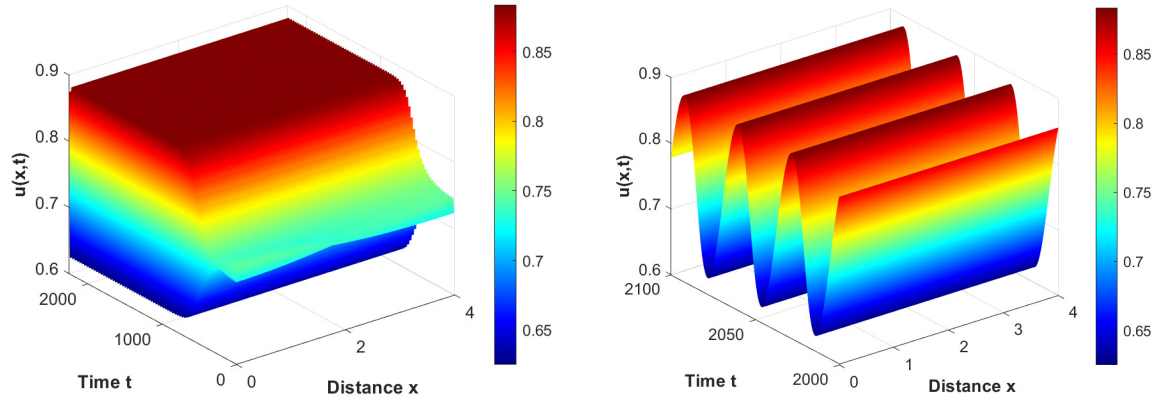

(a) (b)

Figure 15. Numerical simulations for prey population with $p = 0.56$, $\tau = 7.5$, $q = 0.45$, $b = 0.1$, $s = 0.25$, $d_1 = 0.13$ and $d_2 = 0.2$. (a) 2250 iterations, (b) from 2000 iterations to 2100 iterations.

5. Conclusions

In this work, we studied the Hopf bifurcation of a delayed diffusive predator-prey model with a weak Allee effect on prey and a fear effect on predator. By the qualitative analytical theory, we have obtained

the conditions of local stability of a coexisting equilibrium and the existence of a Hopf bifurcation and Turing instable. By using the methods of the normal form theory and center manifold theorem, we have studied the property of the bifurcating periodic solutions. We found that the weak Allee effect and fear effect greatly affected the dynamical behaviour of the new Leslie-Gower model.

First, we discuss the influence of the weak Allee effect. On the whole, the weak Allee effect at a larger value has a great influence on the ecological extinction, controlling stable coexisting equilibrium, and periodic oscillation. Specifically, under the premise that the fear effect remains unchanged, when the weak Allee effect is small, a small increase is not beneficial to the stability of the coexisting equilibrium and will be easy to produce an inhomogeneous periodic solution, which is not conducive to the survival of the population. Thus, when the weak Allee effect increases, either improved defending or hiding of the prey species form the predator may be difficult, and the prey population is generally at a low density. After increasing to a certain extent, the effect will be the completely opposite, and the homogeneity of periodic solutions usually changes from inhomogeneous to homogeneous. The homogeneity is either an invariance or regularity under a particular transformation. Ecologically, the periodic solutions are homogeneous means that the members or parts of prey specie have the same dynamic behavior at all times. Thus, increasing the weak Allee effect to a certain extent undermines this invariance or regularity of the prey species, which is beneficial to the survival of the population. When the weak Allee effect is large, increasing the weak Allee effect will be beneficial to the stability of the coexisting equilibrium and will easily produce a homogeneous periodic solution, which will make the prey population increase their likelihood of extinction.

Finally, we will discuss the influence of the fear effect on population dynamics. Specifically speaking, under the premise that the weak Allee effect remains unchanged, an increase of the fear effect is not beneficial to the stability of the coexisting equilibrium. The homogeneity of periodic solutions usually changes from inhomogeneous to homogeneous, which is conducive to the survival of the population, since the fear effect on predators can protect prey and predators from being eliminated.

Use of AI tools declaration

The authors declare they have not used Artificial Intelligence (AI) tools in the creation of this article.

Acknowledgments

This research is supported by the Fundamental Research Funds for the Central Universities (Grant No. 2572022DJ05), Harbin Science and Technology Bureau Manufacturing Innovation Talent Project (CXRC20221110393), Heilongjiang Science and Technology Department Provincial Key R&D Program Applied Research Project (SC2022ZX06C0025), Heilongjiang Science and Technology Department Provincial Key R&D Program Guidance Project (GZ20220088) and Postdoctoral program of Heilongjiang Province (No. LBHQ21060).

Conflict of interest

The authors have no conflicts of interest to declare. All co-authors have seen and agree with the contents of the manuscript and there is no financial interest to report.

References

1. T. Faria, L. T. Magalhaes, Normal forms for retarded functional differential equations with parameters and applications to Hopf bifurcation, *J. Differ. Equations*, **122** (1995), 181–200. https://doi.org/10.1006/JDEQ.1995.1144
2. T. Faria, Normal forms and Hopf bifurcation for partial differential equations with delays, *Trans. Amer. Math. Soc.*, **352** (2000), 2217–2238. https://doi.org/10.1090/S0002-9947-00-02280-7
3. F. Yi, J. Wei, J. Shi, Bifurcation and spatiotemporal patterns in a homogeneous diffusive predator-prey system, *J. Differ. Equations*, **246** (2009), 1944–1977. https://doi.org/10.1016/J.JDE.2008.10.024
4. B. Messaoud, M. B. Almatrafi, Bifurcation and stability of two-dimensional activator-inhibitor model with fractional-order derivative, *Fractal Fract.*, **7** (2023), 344. https://doi.org/10.3390/fractalfract7050344
5. A. Q. Khan, S. A. H. Bukhari, M. B. Almatrafi, Global dynamics, Neimark-Sacker bifurcation and hybrid control in a Leslie's prey-predator model, *Alexandria Eng. J.*, **61** (2022), 11391–11404. https://doi.org/10.1016/j.aej.2022.04.042
6. A. Q. Khan, F. Nazir, M. B. Almatrafi, Bifurcation analysis of a discrete Phytoplankton-Zooplankton model with linear predational response function and toxic substance distribution, *Int. J. Biomath.*, **16** (2022), 2250095. https://doi.org/10.1142/s1793524522500954
7. A. Q. Khan, M. Tasneem, M. B. Almatrafi, Discrete-time COVID-19 epidemic model with bifurcation and control, *Math. Biosci. Eng.*, **19** (2022), 1944–1969. https://doi.org/10.3934/mbe.2022092
8. J. Li, Y. Song, Spatially inhomogeneous periodic patterns induced by distributed memory in the memory-based single population model, *Appl. Math. Lett.*, **137** (2023), 108490. https://doi.org/10.1016/j.aml.2022.108490
9. H. Shen, Y. Song, H. Wang, Bifurcations in a diffusive resource-consumer model with distributed memory, *J. Differ. Equations*, **347** (2023), 170–211. https://doi.org/10.1016/j.jde.2022.11.044
10. S. Pal, S. Majhi, S. Mandal, N. Pal, Role of fear in a predator-prey model with Beddington-DeAngelis functional response, *Z. Nat. A*, **74** (2019), 581–595. https://doi.org/10.1515/ZNA-2018-0449
11. E. L. Preisser, D. I. Bolnick, The many faces of fear: comparing the pathways and impacts of nonconsumptive predator effects on prey populations, *PLoS ONE*, **3** (2008), e2465. https://doi.org/10.1371/journal.pone.0002465
12. S. Creel, D. Christianson, Relationships between direct predation and risk effects, *Trends Ecol. Evol.*, **23** (2008), 194–201. https://doi.org/10.1016/j.tree.2007.12.004

13. R. Yang, Q. Song, Y. An, Spatiotemporal dynamics in a predator-prey model with functional response increasing in both predator and prey densities, *Mathematics*, **10** (2022), 17. https://doi.org/10.3390/math10010017

14. M. Clinchy, M. J. Sheriff, L. Y. Zanette, Predator-induced stress and the ecology of fear, *Funct. Ecol.*, **27** (2013), 56–65. https://doi.org/10.1111/1365-2435.12007

15. Y. Song, Y. Peng, T. Zhang, The spatially inhomogeneous Hopf bifurcation induced by memory delay in a memory-based diffusion system, *J. Differ. Equations*, **300** (2021), 597–624. https://doi.org/10.1016/J.JDE.2021.08.010

16. X. Wang, L. Y. Zanette, X. Zou, Modelling the fear effect in predator-prey interactions, *J. Math. Biol.*, **73** (2016), 1179–1204. https://doi.org/10.1007/S00285-016-0989-1

17. R. Pringle, T. Kartzinel, T. Palmer, T. J. Thurman, K. Fox-Dobbs, C. C. Y. Xu, et al., Predator-induced collapse of niche structure and species coexistence, *Nature*, **570** (2019), 58–64. https://doi.org/10.1038/s41586-019-1264-6

18. P. Pandy, N. Pal, S. Samanta, J. Chattopadhyay, A three species food chain model with fear induced trophic cascade, *Int. J. Appl. Comput. Math.*, **5** (2019), 100. https://doi.org/10.1007/s40819-019-0688-x

19. J. P. Suraci, M. Clinchy, L. M. Dill, D. Roberts, L. Y. Zanette, Fear of large carnivores causes a trophic cascade, *Nat. Commun.*, **7** (2016), 10698. https://doi.org/10.1038/ncomms10698

20. W. C. Allee, A. Aggregations, *A study in general sociology*, University of Chicago Press, 1931. https://doi.org/10.2307/2961735

21. T. Liu, L. Chen, F. Chen, Z. Li, Dynamics of a Leslie-Gower model with weak Allee effect on prey and fear effect on predator, *Int. J. Bifurcation Chaos*, **33** (2023), 2350008. https://doi.org/10.1142/s0218127423500086

22. J. Jiao, C. Chen, Bogdanov-Takens bifurcation analysis of a delayed predator-prey system with double Allee effect, *Nonlinear Dyn.*, **104** (2021), 1697–1707. https://doi.org/10.1007/s11071-021-06338-x

23. P. Aguirre, A general class of predation models with multiplicative Allee effect, *Nonlinear Dyn.*, **78** (2014), 629–648. https://doi.org/10.1007/S11071-014-1465-3

24. F. Courchamp, T. Clutton-Brock, B. Grenfell, F. Courchamp T. Clutton-Brock, B. Grenfell, et al., Inverse density dependence and the Allee effect, *Trends Ecol. Evol.*, **14** (1999), 405–410. https://doi.org/10.1016/S0169-5347(99)01683-3

25. P. Feng, Y. Kang, Dynamics of a modified Leslie-Gower model with double Allee effects, *Nonlinear Dyn.*, **80** (2015), 1051–1062. https://doi.org/10.1007/S11071-015-1927-2

26. N. Iqbal, R. Wu, Turing patterns induced by cross-diffusion in a 2D domain with strong Allee effect, *C. R. Math.*, **357** (2019), 863–877. https://doi.org/10.1016/j.crma.2019.10.011

27. D. S. Boukal, L. Berec, Modelling mate-finding Allee effects and populations dynamics, with applications in pest control, *Popul. Ecol.*, **51** (2009), 445–458. https://doi.org/10.1007/s10144-009-0154-4

28. M. H. Wang, M. Kot, Speeds of invasion in a model with strong or weak Allee effects, *Math. Biosci.*, **171** (2001), 83–97. https://doi.org/10.1016/S0025-5564(01)00048-7

29. T. Liu, L. Chen, F. Chen, Z. Li, Stability analysis of a Leslie-Gower model with strong Allee effect on prey and fear effect on predator, *Int. J. Bifurcation Chaos*, **32** (2022), 2250082. https://doi.org/10.1142/S0218127422500821

30. K. Fang, Z. L. Zhu, F. D. Chen, Z. Li, Qualitative and bifurcation analysis in a Leslie-Gower model with Allee effect, *Qual. Theory Dyn. Syst.*, **21** (2022), 86. https://doi.org/10.1007/s12346-022-00591-0

31. L. M. Zhang, Y. K. Xu, G. Y. Liao, Codimension-two bifurcations and bifurcation controls in a discrete biological system with weak Allee effect, *Int. J. Bifurcation Chaos*, **32** (2022), 2250036. https://doi.org/10.1142/s0218127422500365

32. L. Zhao, J. H. Shen, Relaxation oscillations in a slow-fast predator-prey model with weak Allee effect and Holling-IV functional response, *Commun. Nonlin. Sci. Numer. Simul.*, **112** (2022), 106517. https://doi.org/10.1016/j.cnsns.2022.106517

33. R. Yang, X. Zhao, Y. An, Dynamical analysis of a delayed diffusive predator-prey model with additional food provided and anti-predator behavior, *Mathematics*, **10** (2022), 469. https://doi.org/10.3390/math10030469

34. W. Zuo, J. Wei, Stability and Hopf bifurcation in a diffusive predator-prey system with delay effect, *Nonlinear Anal.: Real World Appl.*, **12** (2011), 1998–2011. https://doi.org/10.1016/J.NONRWA.2010.12.016

35. R. Yang, D. Jin, W. Wang, A diffusive predator-prey model with generalist predator and time delay, *AIMS Math.*, **7** (2022), 4574–4591. https://doi.org/10.3934/math.2022255

36. J. F. Zhang, X. P. Yan, Effects of delay and diffusion on the dynamics of a Leslie-Gower type predator-prey model, *Int. J. Bifurcation Chaos*, **24** (2014), 1450043. https://doi.org/10.1142/S0218127414500436

37. Y. Song, Y. Peng, T. Zhang, Double Hopf bifurcation analysis in the memory-based diffusion system, *J. Dyn. Differ. Equ.*, 2022. https://doi.org/10.1007/s10884-022-10180-z

38. M. U. Akhmet, M. Beklioglu, T. Ergenc, V. I. Tkachenko, An impulsive ratio-dependent predator-prey system with diffusion, *Nonlinear Anal.: Real World Appl.*, **7** (2006), 1255–1267. https://doi.org/10.1016/j.nonrwa.2005.11.007

39. Y. Liu, J. Wei, Double Hopf bifurcation of a diffusive predator-prey system with strong Allee effect and two delays, *Nonlinear Anal.: Model. Control*, **26** (2021), 72–92. https://doi.org/10.15388/namc.2021.26.20561

40. Y. Liu, D. Duan, B. Niu, Spatiotemporal dynamics in a diffusive predator-prey model with group defense and nonlocal competition, *Appl. Math. Lett.*, **103** (2019), 106175. https://doi.org/10.1016/j.aml.2019.106175

41. R. Yang, F. Wang, D. Jin, Spatially inhomogeneous bifurcating periodic solutions induced by nonlocal competition in a predator-prey system with additional food, *Math. Methods Appl. Sci.*, **45** (2022), 9967–9978. https://doi.org/10.1002/mma.8349

42. S. Chen, J. Yu, Stability and bifurcation on predator-prey systems with nonlocal prey competition, *Discrete Contin. Dyn. Syst.*, **38** (2018), 43–62. https://doi.org/10.3934/DCDS.2018002

43. R. Yang, C. Nie, D. Jin, Spatiotemporal dynamics induced by nonlocal competition in a diffusive predator-prey system with habitat complexity, *Nonlinear Dyn.*, **110** (2022), 879–900. https://doi.org/10.1007/s11071-022-07625-x

44. D. Geng, W. Jiang, Y. Lou, H. Wang, Spatiotemporal patterns in a diffusive predator-prey system with nonlocal intraspecific prey competition, *Stud. Appl. Math.*, **148** (2021), 396–432. https://doi.org/10.1111/sapm.12444

45. M. G. Clerc, D. Escaff, V. M. Kenkre, Analytical studies of fronts, colonies, and patterns: combination of the Allee effect and nonlocal competition interactions, *Phys. Rev. E*, **82** (2010), 036210. https://doi.org/10.1103/PHYSREVE.82.036210

46. Y. E. Maruvka, T. Kalisky, N. M. Shnerb, Nonlocal competition and the speciation transition on random networks, *Phys. Rev. E*, **78** (2008), 031920. https://doi.org/10.1103/PHYSREVE.78.031920

47. N. F. Britton, Aggregation and the competitive exclusion principle, *J. Theor. Biol.*, **136** (1989), 57–66. https://doi.org/10.1016/S0022-5193(89)80189-4

48. J. Furter, M. Grinfeld, Local vs. non-local interactions in population dynamics, *J. Math. Biol.*, **27** (1989), 65–80. https://doi.org/10.1007/BF00276081

AIMS Press